JOURNAL OF SOLID STATE CHEMISTRY 109, 15–21 (1994)

Conductivity Enhancement in NaCl by Dispersion of Al_2O_3

Ashok Kumar and K. Shahi

Materials Science Programme, Indian Institute of Technology, Kanpur-208016, India

Received November 2, 1992; in revised form May 20, 1993; accepted May 21, 1993

The composite solid electrolytes NaCl-x mole% Al_2O_3 ($0 \leq x \leq 50$) have been prepared by conventional as well as solution casting methods and have been investigated by means of complex impedance analysis, X-ray diffraction (XRD), differential thermal analysis (DTA), and scanning electron microscopy (SEM). The composites prepared by conventional method exhibit about an order of magnitude lower conductivity than those prepared by solution casting technique. The XRD and DTA results show that no phases other than NaCl and Al_2O_3 are present. SEM results show that NaCl grains are interspersed with Al_2O_3 particles. The conductivity of dispersed systems depends on the processing and the particle size and concentration of Al_2O_3. The mechanism of excess conductivity is proposed to be the generation of excess sodium ion vacancies in the host matrix at the matrix–particle interface. Macroscopically, the results are satisfactorily explained on the basis of random resistor network model by assuming the formation of high conducting space charge layer along the matrix–particle interface.

1. INTRODUCTION

Since the discovery of ionic conductivity enhancement in LiI due to dispersion of Al_2O_3 (1), considerable attention has been devoted to the study of conductivity in composite solid electrolytes (2–10). The conduction in such electrolytes is different from that in the conventional homogeneously doped ones in that the fulfillment of local electroneutrality condition is decisive in the latter whereas in the case of former interfaces are utilized to give rise to high ionic conductivity and the deviations from electroneutrality at the matrix–particle interface are important (6). Superionic conductors such as α-AgI, however, show decrease in ionic conductivity due to dispersion of insulating particle such as Al_2O_3, SiO_2, CeO_2, etc. (11).

The composite solid electrolytes have become important to both scientists and technologists. To understand the mechanism responsible for the enhanced conductivity, emphasis has been laid on matrix–particle interfaces. Almost all the models proposed (12–18) assume the formation of highly conducting space charge layer along the interface. Besides ionic conductivity enhancement some other interesting phenomena have also been observed. For instance it has been found from NMR experiments that due to dispersion of Al_2O_3 in LiCl an additional peak appears and overlaps the NMR absorption line (11).

Even though the studies on composite solid electrolytes are numerous and vigorous, the alkali halide based composites, with the exception of lithium salts, have not been investigated. This paper reports the synthesis of NaCl–Al_2O_3 composites and their structural and electrical characterization studies. NaCl was chosen as the matrix material because it (i) is not very hygroscopic, (ii) does not exhibit any solid-solid transformation, and (iii) is well understood with regard to its defect and conduction mechanisms. Thus the effect of Al_2O_3 dispersion can be studied over a wide temperature range which should be helpful in identifying the mechanism of enhanced conductivity in composites.

2. EXPERIMENTAL

The high purity NaCl was obtained from the Aldrich Chemicals, Inc. and the deagglomerated Al_2O_3 powder of three different initial particle sizes (0.05, 0.3, and 1.0 μm) was obtained from Buehler Micropolish II. The samples of NaCl–Al_2O_3 were prepared by two different methods. In the conventional method the samples were prepared by thoroughly mixing appropriate amounts of the two components in an agate pestle and mortar, followed by heating the mixture above the melting point (≈850°C) of NaCl for several hours to ensure a homogeneous dispersion of Al_2O_3 particles in NaCl, and finally cooling in the furnace. The powder thus obtained was reground and pelletized in a 9 mm diameter die at pressure of 6 ton/cm^2. The pellets were subsequently sintered at 770°C for 24 hr. In the solution casting method NaCl was dissolved in distilled water and an appropriate amount of Al_2O_3 was added to the solution. The solution was then magnetically stirred and simultaneously evaporated. The solid chunk thus prepared was ground and pelletized in the same way as those prepared by conventional method.

Platinum in the form of paint followed by curing at

0022-4596/94 $6.00

160°C for 1 hr was used as electrodes for electrical measurements. The ac impedance data $|z|$ and θ were obtained by using an HP 4192A impedance analyzer over temperature range 600 to 200°C during cooling cycle at a step of 20–25°C. To analyze the ac impedance data an integrated software package (19), which also provides for automatic data entry, acquisition, and analysis was used. Sufficient time (about 30 min) was allowed at each temperature for equilibration. The temperature of the furnace was controlled to within ±1°C by means of a PID temperature controller (Indotherm 401-D).

The XRD patterns were recorded at room temperature by using Rich-Seifert (Iso-Debye Flex 2002D) Counter diffractometer that employs Cu$K\alpha$ radiation. The DTA measurements were carried out using mini DTA (Linseis L 62) with a heating/cooling rate of 5°C per minute. Jeol model JSM-840A scanning electron microscope was used to examine the distribution of Al_2O_3 particle.

Even though the particle sizes of Al_2O_3 were quoted by the manufacturers to be 0.05, 0.3, and 1.0 μm the particles were expected to be larger due to agglomeration. Besides, the agglomeration of Al_2O_3 may occur in various stages of sample processing. Thus the particle sizes were subsequently measured by Coulter counter model Z_B and B, and SEM, and found to have values of 1.2, 2.9, and 5.7 μm respectively. The particle sizes determined by SEM were found to be in broad agreement with the above results. The specific surface area of the particles obtained by BET technique was 11.38, 3.35, and 2.74 m^2/g respectively.

3. RESULTS AND DISCUSSION

3.1. *X-Ray Diffraction*

Figure 1 shows the X-ray diffractograms of NaCl–40 mole% Al_2O_3 composition before and after heating the mixture at 750°C. These results show no evidence of any chemical reaction or solid solution formation between Al_2O_3 and NaCl.

3.2. *Differential Thermal Analysis*

Figure 2 shows the DTA traces of NaCl–40 mole% Al_2O_3 composition before and after heating the mixture at 750°C. The peak in both the curves corresponds to the melting of NaCl, thereby ruling out the possibility of any chemical reaction or solid solution formation between Al_2O_3 and NaCl.

3.3. *Scanning Electron Microscopy*

The scanning electron micrographs of pure NaCl and NaCl–30 mole% Al_2O_3 sintered at 750°C are shown in Fig. 3. In case of pure NaCl (Fig. 3a) it was observed that the polycrystalline grains are uniformly distributed whereas in case of NaCl–30 mole% Al_2O_3 (Fig. 3b) the NaCl grains are interspersed with Al_2O_3 particles.

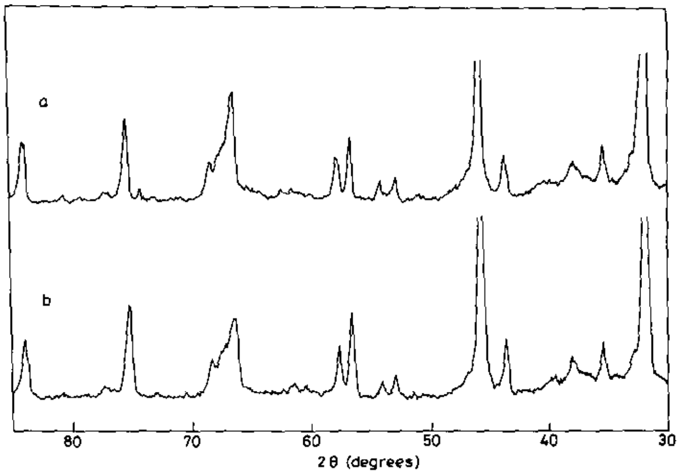

FIG. 1. The X-ray diffraction patterns for (a) preheated and (b) postheated NaCl–40 mole% Al_2O_3 at 750°C.

3.4. *Electrical Conductivity*

The conductivity for all the samples at each temperature was obtained from the complex impedance analysis. The high frequency semicircular portion of the impedance spectra could be expressed as a constant phase element in parallel with the bulk resistance. The resistance of the high-frequency semicircular portion has been used to calculate the conductivity for various composites.

3.4.1. *Electrical conductivity vs composition.* Fig-

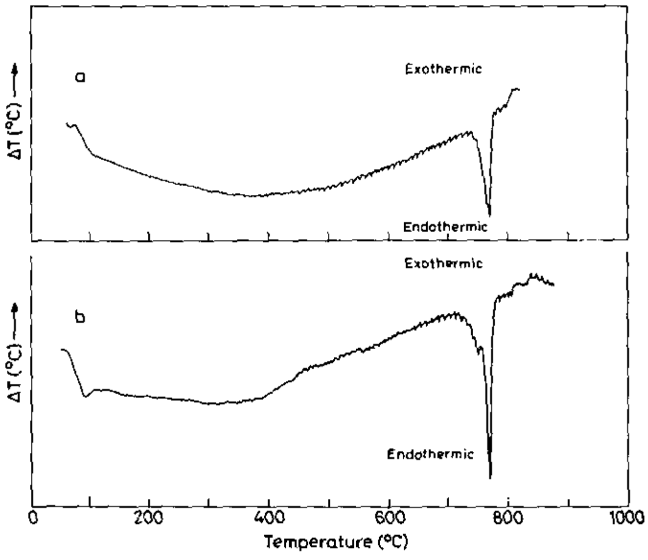

FIG. 2. The differential thermal analysis plots for (a) preheated and (b) postheated NaCl–40 mole% Al_2O_3 at 750°C.

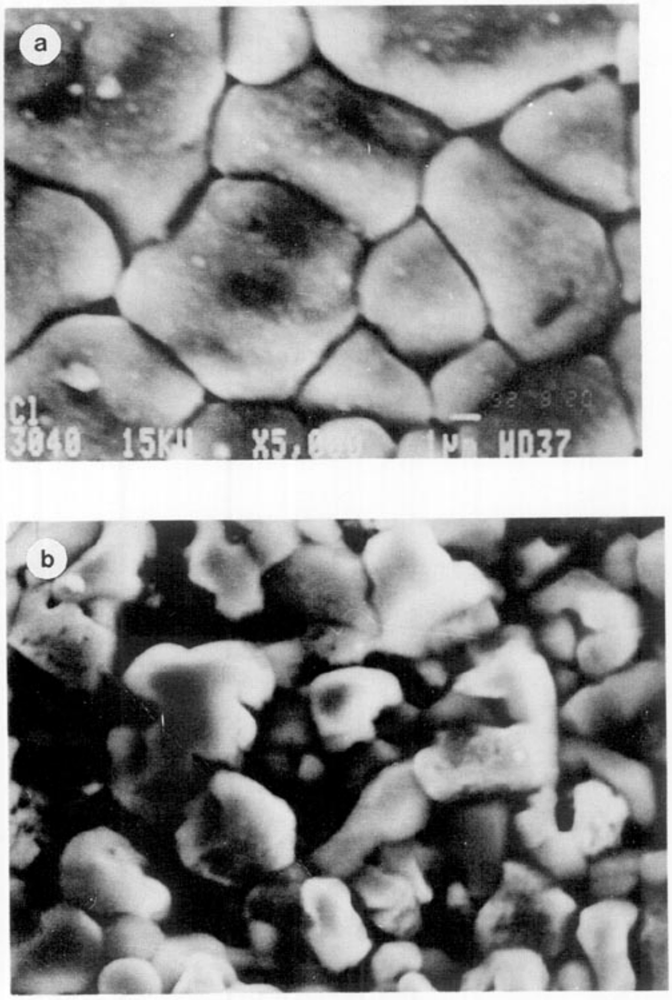

FIG. 3. The scanning electron micrographs for (a) polycrystalline NaCl and (b) NaCl dispersed with 30 m/o Al_2O_3.

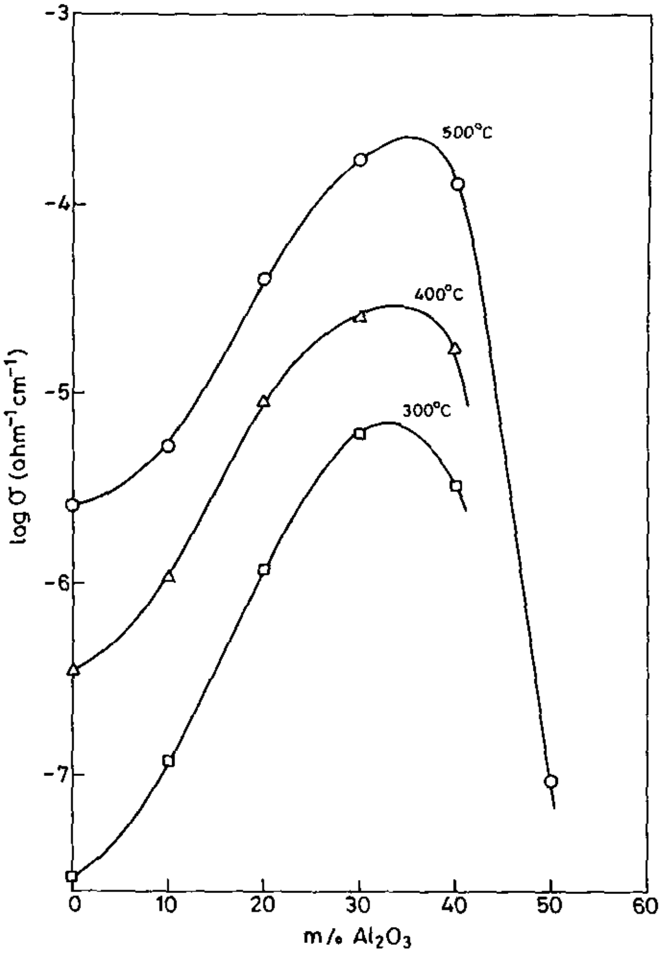

FIG. 4. The variation of conductivity as a function of composition (mole% Al_2O_3) at three different temperatures.

ure 4 shows the variation of electrical conductivity as a function of concentration (mole%) of Al_2O_3 in NaCl at three different temperatures viz., 300, 400, and 500°C. The conductivity increases sharply as the concentration of Al_2O_3 increases, attains a maximum value at $\simeq$35 mole% Al_2O_3 and starts decreasing subsequently. Table 1 compares the normalized conductivity of NaCl–Al_2O_3 composites at 300, 400, and 500°C. The data show that the enhancement in conductivity is by two orders of magnitude for NaCl–30 mole% Al_2O_3 composite system and is more pronounced at lower temperatures for any given composite. These features are in general similar to those of other composite systems (2–9). Table 2 compares the normalized conductivity of NaCl–30 mole Al_2O_3 samplès prepared by conventional and solution casting methods.

It is observed that the enhancement in conductivity for a given composite is generally more for the sample prepared by solution casting than by the conventional method. This may be due to combined effects of more uniform distribution of particles as well as chemisorbed water on the surface of the dispersoids. Thus these results reinforce the existing view (3, 15) that the wet Al_2O_3 is more effective than the dry Al_2O_3 and that the matrix–

TABLE 1

Normalized Conductivity (σ/σ^0) of NaCl–Al_2O_3 Composites of Various Compositions at Three Different Temperatures

Composition (m/o Al_2O_3)	σ/σ^0 (300°C)	(400°C)	(500°C)
0	1	1	1
10	4	3	2
20	40	25	16
30	220	114	72
40	115	77	52
50	—	—	4×10^{-2}

TABLE 2

Normalized Conductivity (σ^{30}/σ^{0}) of NaCl–30 mole% Al_2O_3 Composites Prepared by Conventional and Solution Casting Methods

Composite type	σ^{30}/σ^{0} (300°C)	(400°C)	(500°C)
Conventional	220	114	72
Solution casting	2.5×10^3	704	316

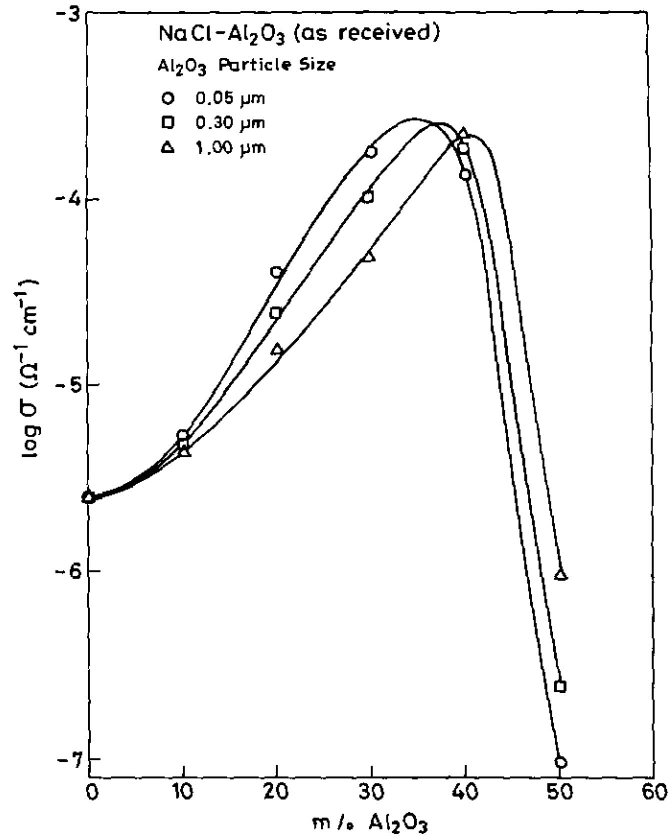

FIG. 5. Composition and particle size dependences of electrical conductivity at 500°C for NaCl–Al_2O_3 composite system.

particle interface plays a dominant role in conductivity enhancement.

The existence of space charge region near lattice discontinuities (free surface, dislocations, and grain boundaries) in an ionic solid was first proposed by Frenkel (23) and the space charge distribution profiles have been formulated by several researchers (24–27). The origin of space charge is ascribed to the difference in the free energy of formation of the individual vacancies in case of Schottky disorder and of the vacancy and the interstitial in case of Frenkel disorder. If there is a chemically inert phase as a second phase instead of vacuum, which means there is no solubility or a global chemical reaction with the crystal, then the space charge profile can be obtained in a similar way as for a crystal in contact with vacuum. Jow and Wagner (14) were the first to use these concepts and proposed that fine dispersoids form well defined space charge regions in contact with the host electrolyte. The space charge profiles for two phase composites have been formulated by Maier (6, 7). According to him, the dispersoid acts as a nucleophilic surface which attracts positively charged species leaving a space charge region of cation vacancies in the host crystal at the interface. An increase in defect concentration in the space charge region gives rise to the excess conductivity in the composite systems.

In pure NaCl crystal at the free surface the formation energy of Na^+ vacancy is lower than that of Cl^- vacancy. As a consequence just beneath the surface there are more cation than anion vacancies resulting in a negative space charge region. If there is a second insoluble (Al_2O_3) phase instead of vacuum, one would expect the increased rate of cation disorder reaction. Consequently sodium ions will be enriched at the interface and the concentration of sodium ion vacancies increases in the host crystal which gives rise to the excess conductivity in NaCl–Al_2O_3 composite systems.

The random resistor network (RRN) model (16–18) which assumes the existence of a highly conducting layer between a normally conducting matrix and a nonconducting dispersoid from the macroscopic point of view and predicts the existence of two critical concentrations, namely, p'_c and p''_c. At p'_c the high conducting layers begin to form connected pathways and at p''_c the connected pathways get disrupted as they begin to form closed loops due to increased concentrations of insulating bonds. The results in Fig. 4 show that the conductivity rises rather rapidly initially, passes through a maximum at ~35 mole% Al_2O_3 and subsequently drops suddenly and thus appears to be inconsistent with the random resistor network model.

The above description of RRN model also qualitatively explains the dependence of conductivity on the particle size of Al_2O_3 (Fig. 5). The finer particles have higher surface area for a given concentration (mole%) of Al_2O_3, and thus the optimum interface required for maximum conductivity is attained at a lower concentration for finer Al_2O_3 particles. The results of Fig. 5 show that the conductivity peak shifts to the right (i.e., higher concentration of Al_2O_3) as particle size increases (i.e., surface area decreases) and are thus consistent with the RRN model.

3.4.2. Electrical conductivity vs particle size. Figure 6 shows log(σ) vs particle size of Al_2O_3 for NaCl–30 mole% Al_2O_3 composite at three different temperatures 300, 400, and 500°C. It is evident that as the particle size of dispersoid increases the relative enhancement in

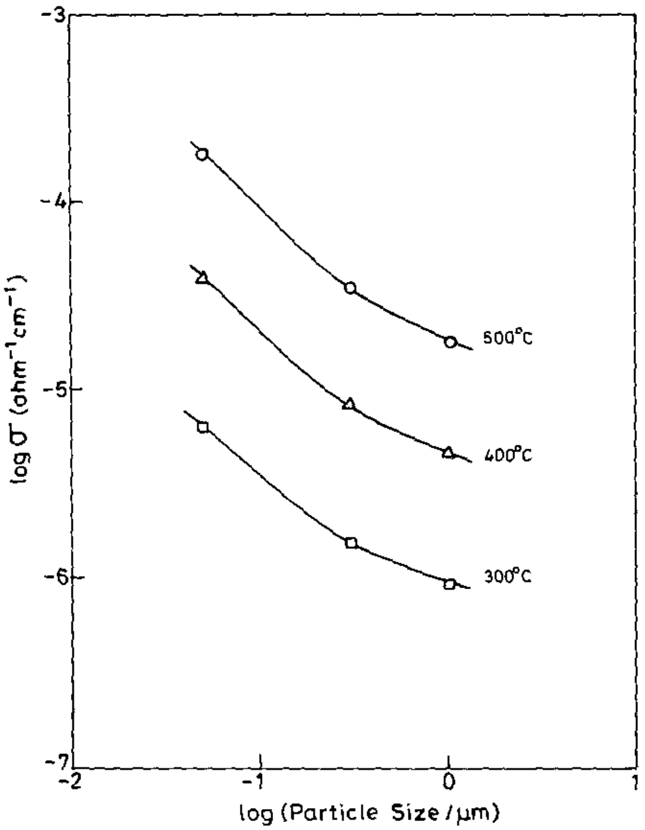

FIG. 6. The variation of conductivity as a function of particle size of Al_2O_3 at different temperatures for NaCl-30 m/o Al_2O_3 composite.

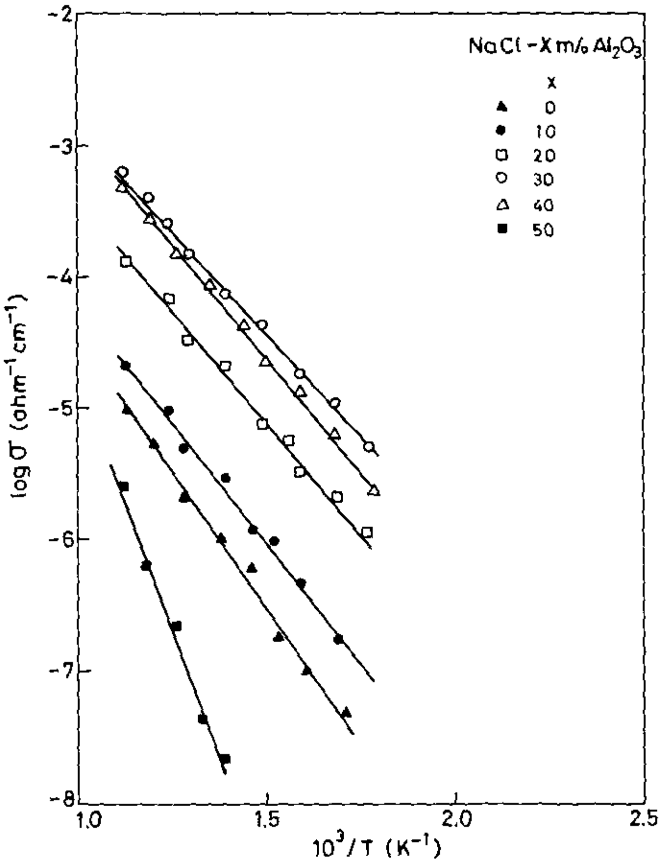

FIG. 7. The variation of conductivity as function of inverse temperature for various NaCl–Al_2O_3 composites.

conductivity decreases rather rapidly but tends to level off at larger values of particle size. Table 3 compares the normalized conductivity of NaCl–30 mole% composite system for three different particle sizes. These results are in general agreement with the general trend reported previously (2–6) on a variety of composite systems.

Several models (12–15) proposed to explain the observed dependence of the enhancement in conductivity on the particle size describe rather empirically the conductivity enhancement as a function of inverse of radius of dispersoid. However, recent studies have emphasized the correlation between the increase in conductivity with increases in effective surface area of dispersed phase (22). For larger particles the surface area per unit volume available for forming high conductivity layers will be smaller causing less enhancement in conductivity.

TABLE 3

Normalized Conductivity (σ/σ^0) of NaCl–30, mole% Al_2O_3 for Different Particle Sizes of Al_2O_3 (0.05, 0.3, and 1.0 μm) at Three Different Temperatures

Size of Al_2O_3 (μm)	σ^{30}/σ^0 (300°C)	(400°C)	(500°C)
0.05	220	114	72
0.3	55	25	14
1.0	32	13	7

3.4.3. Electrical conductivity vs temperature. The log(σ) versus $10^3/T$ behavior for various NaCl–Al_2O_3 composites is shown in Fig. 7. The transport parameters, viz., the preexponential factor (σ_0) and the activation energy (E_a) are given in Table 4. It evident from the results that the effect of dispersion is to enhance the conductivity. These results are consistent with the results reported earlier (2–14) for various composite systems.

It is conceivable that the excess conductivity may be ascribed to the excess sodium vacancies generated by dissolution of Al_2O_3 molecules in sodium chloride lattice as follows:

$$Al_2O_3 \leftrightarrow 2Al_{Na}^{\cdot\cdot} + V'_{Na} + 3O'_{Cl},$$

where the Kröger-Vink notation has been used. Thus

TABLE 4

Ionic Transport Parameters viz. the Preexponential Factor (σ_0) and the Activation Energy (E_a) of NaCl–Al_2O_3 Composites Prepared by Conventional Methods

Mole% of Al_2O_3 in NaCl	Temperature range (°C)	E_a (eV)	σ_0 (S/cm)
0	300–600	0.82	4.8×10^{-1}
10	300–600	0.72	2.6×10^{-1}
20	300–600	0.68	1.1
30	300–600	0.62	1.7
40	300–600	0.69	3.9
50	450–600	1.53	9.3×10^2

one molecule of dissolved Al_2O_3 produces one excess sodium ion vacancy. If this were the mechanism of conductivity enhancement a simple calculation, using known mobility value of Na ion vacancy at 300°C (30), would suggest that a fraction of a mole% of the dopant (Al_2O_3) is required to achieve the observed conductivity of $\sim 10^{-5}$ S/cm at 300°C. On the other hand, the experiments show that there is very little enhancement in the conductivity due to addition of as large as 10 mole% Al_2O_3 and that the maximum enhancement in conductivity occurs at $\approx$35 mole% Al_2O_3. This clearly suggests that the classical doping mechanism cannot explain the conductivity enhancement in NaCl–Al_2O_3 composite system. It is also conceivable that dispersion of alumina increases the dislocation density in the host matrix and the excess space charge at the dislocations may contribute to the excess conductivity. In addition, the phenomena involving matrix may also contribute to the conductivity enhancement (20, 21). However, the dependence of conductivity on the processing and particle size indicates that the mechanism responsible for conductivity enhancement must involve the matrix–particle interface. The activation energy for various NaCl–Al_2O_3 composites is comparable to sodium ion vacancy migration enthalpy reported for pure NaCl (28, 29). This is in accordance with the space charge theory that the excess sodium ion vacancies are induced in the matrix at the interface.

Figure 8 compares the log (σ) versus $10^3/T$ plot for NaCl–30 mole% Al_2O_3 prepared by the conventional method and by solution casting methods. The samples prepared by the latter method show about an order of magnitude higher enhancement in conductivity as compared to those prepared by conventional method. This result further indicates that the enhancement in conductivity could be due to water chemisorbed on the Al_2O_3 surface. This result is consistent with the space charge theory. The presence of chemical species such as water at the interface may increase the cation disorder reaction giving rise to higher concentration of sodium ion vacancies than in case of dry Al_2O_3 particles.

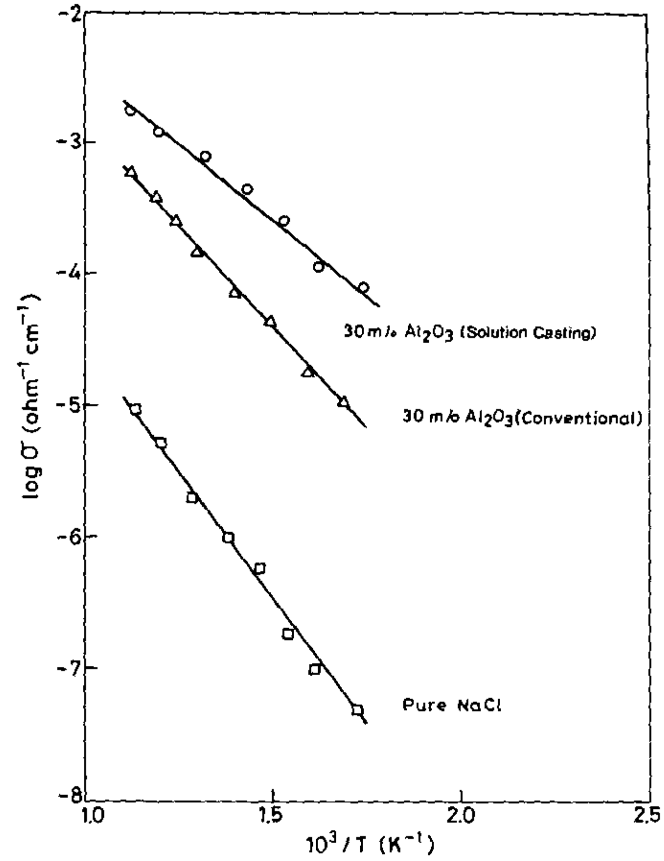

FIG. 8. The variation of conductivity as a function of inverse temperature for NaCl–30 m/o Al_2O_3 composite prepared by conventional and solution casting method.

CONCLUSIONS

NaCl containing dispersed Al_2O_3 particles exhibits enhanced electrical conductivity. That the interface between NaCl matrix and Al_2O_3 particles contributes to this effect has been explained by processing (conventional and solution casting methods), particle size and compositional dependences of conductivity. The NaCl–30 mole% Al_2O_3 prepared by solution casting method shows conductivity $\sim 10^{-4}$ S/cm at 300°C which is more than three orders of magnitude higher than that for pure NaCl at that temperature, and an order of magnitude larger than that of the same composite but prepared by the conventional method.

REFERENCES

1. C. C. Liang, *J. Electrochem. Soc.* **120,** 1289 (1973).
2. J. B. Wagner, Jr., *Mater. Res. Bull.* **15,** 1691 (1980).
3. K. Shahi and J. B. Wagner, Jr., *J. Electrochem. Soc.* **128,** 6 (1981).

4. O. Nakamura and J. B. Goodenough, *Solid State Ionics* **7,** 119 (1982).
5. M. R-W. Chang, K. Shahi and J. B. Wagner, Jr., *J. Electrochem. Soc.* **131,** 1213 (1984).
6. J. Maier, *J. Phys. Chem. Solids* **46,** 309 (1985).
7. J. Maier, *Ber. Bunsenges. Phys. Chem.* **89,** 355 (1986).
8. N. Vaidehi, R. Akila, A. K. Shukla and K. T. Jacob, *Mater. Res. Bull.* **21,** 909 (1986).
9. S. Fijitsu, K. Koumota and H. Yanagida, *Solid State Ionics* **18/19,** 1146 (1986).
10. A. K. Shukla, R. Manoharan and J. B. Goodenough, *Solid State Ionics* **26,** 5 (1986).
11. Chen Liquan, *in* "Materials for Solid State Batteries" (B. V. R. Chowdhari and S. Radhakrishna, Eds.), p. 69. World Scientific, Singapore, 1986.
12. C. Wagner, *J. Phys. Chem. Solids* **33,** 1051 (1972).
13. A. M. Stoneham, Evelyn Wade and J. A. Kilner, *Mater. Res. Bull.* **14,** 661 (1979).
14. T. Jow and J. B. Wagner, Jr., *J. Electrochem. Soc.* **126,** 1963 (1979).
15. S. Pack, "Electrical Conductivity of HgI_2 Containing Al_2O_3 particles," Abstract 133. Electrochemical Society Meeting, Los Angeles, October 1979.
16. A. Bunde, W. Dieterich and H. E. Roman, *Phys. Rev. Lett.* **55,** 5 (1985).
17. H. E. Roman, A. Bunde and W. Dieterich, *Phys. Rev. B* **34,** 3439 (1986).
18. H. E. Roman and M. Yussouff, *Phys. Rev. B* **36,** 7285 (1987).
19. S. Bhatnagar, S. Gupta and K. Shahi, *Solid State Ionics* **31,** 107 (1988).
20. N. J. Dudney, *J. Am. Ceram. Soc.* **75,** 65 (1987).
21. T. L. Wen, R. A. Huggins, A. Rabenau and W. Weppner, *Rev. Chim. Miner.* **20,** 643 (1983).
22. C. T. Slade and I. M. Thompson, *Solid State Ionics* **26,** 287 (1988).
23. J. Frenkel, "Kinetic theory of liquids," p. 36. Oxford Univ. Press, New York, 1946.
24. K. Lehovec, *J. Chem. Phys.* **21,** 1123 (1953).
25. K. L. Kliewer and J. S. Koehler, *Phys. Rev.* **140,** A 1226 (1965).
26. J. D. Eshelby, W. A. Newey, P. L. Pratt and A. B. Lidiard, *Philos. Mag.* **8,** 75 (1958).
27. M. F. Yan, R. M. Cannon, H. K. Bowen and R. L. Coble, *J. Am. Ceram. Soc.* **60,** 120 (1977).
28. R. W. Dreyfus and A. S. Nowick, *Phys. Rev.* **126,** 1367 (1962).
29. R. W. Dreyfus and A. S. Nowick, *J. Appl. Phys.* **33,** 473 (1962).
30. H. W. Etzel and R. J. Maurer, *J. Chem. Phys.* **18,** 1003 (1950).